Subunit-specific gating controls rat NR1/NR2A and NR1/NR2B NMDA channel kinetics and synaptic signalling profiles

Kevin Erreger[1], Shashank M. Dravid[1], Tue G. Banke[1], David J. A. Wyllie[2] and Stephen F. Traynelis[1]

[1]*Department of Pharmacology, Emory University School of Medicine, Rollins Research Center, Atlanta, GA 30322-3090, USA*
[2]*Division of Neuroscience, University of Edinburgh, 1 George Square, Edinburgh EH8 9JZ, UK*

NR2A and NR2B are the predominant NR2 NMDA receptor subunits expressed in cortex and hippocampus. The relative expression level of NR2A and NR2B is regulated developmentally and these two subunits have been suggested to play distinct roles in long-term synaptic plasticity. We have used patch-clamp recording of recombinant NMDA receptors expressed in HEK293 cells to characterize the activation properties of both NR1/NR2A and NR1/NR2B receptors. Recordings from outside-out patches that contain a single active channel show that NR2A-containing receptors have a higher probability of opening at least once in response to a brief synaptic-like pulse of glutamate than NR2B-containing receptors (NR2A, 0.80; NR2B, 0.56), a higher peak open probability (NR2A, 0.50; NR2B, 0.12), and a higher open probability within an activation (NR2A, 0.67; NR2B, 0.37). Analysis of the sequence of single-channel open and closed intervals shows that both NR2A- and NR2B-containing receptors undergo multiple conformational changes prior to opening of the channel, with at least one of these steps being faster for NR2A than NR2B. These distinct properties produce profoundly different temporal signalling profiles for NR2A- and NR2B-containing receptors. Simulations of synaptic responses demonstrate that at low frequencies typically used to induce long-term depression (LTD; 1 Hz), NR1/NR2B makes a larger contribution to total charge transfer and therefore calcium influx than NR1/NR2A. However, under high-frequency tetanic stimulation (100 Hz; $>$ 100 ms) typically used to induce long-term potentiation (LTP), the charge transfer mediated by NR1/NR2A considerably exceeds that of NR1/NR2B.

(Received 24 November 2004; accepted after revision 7 January 2005; first published online 13 January 2005)
Corresponding author K. Erreger: Department of Molecular Biophysics & Physiology, Vanderbilt University, 7124 MRB III, Nashville, TN 37232, USA. Email: kevin.erreger@vanderbilt.edu

The NMDA subtype of ionotropic glutamate receptors comprises both NR1 and NR2 receptor subunits and plays a major role in both physiological and pathophysiological processes in the brain (reviewed by Dingledine *et al.* 1999; Cull-Candy *et al.* 2001), as well as being a promising therapeutic target (reviewed by Brauner-Osborne *et al.* 2000). The identity of the NR2 subunit (NR2A–D) strongly influences the pharmacological and biophysical properties of the receptor (Williams *et al.* 1994; Sucher *et al.* 1996; Krupp *et al.* 1998; Paoletti *et al.* 2000; reviewed by Erreger *et al.* 2004). While the NR1 subunit is expressed ubiquitously, expression patterns of NR2 subunits are regulated both spatially and temporally. For example, in the cortex and hippocampus the NR2B subunit is predominantly expressed early in development, whereas expression of the NR2A subunit increases over time resulting in a developmental shift in functional properties of NMDA receptors (Hestrin, 1992; Monyer *et al.* 1994; Sheng *et al.* 1994; Flint *et al.* 1997; reviewed by van Zundert *et al.* 2004). Activity-dependent changes in the synaptic density of NR2A and NR2B have also been described (Fujisawa & Aoki, 2003; Ehlers, 2003). Synaptic and extrasynaptic NMDA receptors have distinct subunit compositions and functional roles (Rumbaugh & Vicini, 1999; Tovar & Westbrook, 1999; Li *et al.* 2002; van Zundert *et al.* 2004). Recent studies have also shown that NR2 subunits make distinct contributions to different forms of long-term synaptic plasticity (Hrabetova *et al.* 2000; Yoshimura *et al.* 2003), with activation of NR2B proposed to induce long-term depression (LTD) and activation of NR2A proposed to induce long-term potentiation (LTP) (Liu *et al.* 2004; Massey *et al.* 2004). These data suggest that there is developmental and activity-dependent regulation of the relative expression and distribution of the NR2A and NR2B subunits, as well as unique physiological roles for each NR2 subunit. Therefore understanding

 DOI: 10.1113/jphysiol.2004.080028

the fundamental functional differences between NMDA receptors containing the NR2A or NR2B subunit will yield insight into multiple aspects of synaptic function.

Several functional differences between NR2A- and NR2B-containing receptors have previously been described. For example, following brief applications of glutamate, NR2B-containing receptors deactivate more slowly than NR2A-containing receptors (Vicini *et al.* 1998) while excitatory post-synaptic currents (EPSCs) mediated by NMDA receptors comprising mainly of NR2B receptor subunits also show slower decays compared to NR2A-containing receptors (Flint *et al.* 1997). These data suggest that NR2B expression allows for greater temporal integration of non-synchronous synaptic inputs, which may explain in part why the NR2B subunit is critical for the development of the nervous system (Kutsuwada *et al.* 1996). Estimates of peak open probability using the open channel blocker MK-801 have suggested that receptors containing the NR2A subunit have a 2- to 5-fold higher peak open probability (P_o) than NR2B (Chen *et al.* 1999). At the single-channel level, NMDA channels exhibit complex kinetic behaviour that depends on the identity of the NR2 subunit (reviewed by Erreger *et al.* 2004).

In this study, we analyse single-channel currents from receptors containing either the NR2A or NR2B subunits to gain insight into how channel gating is regulated by the NR2 subunit. Our analyses suggest that there are multiple activating conformational changes preceding channel opening and that at least one of these pre-gating steps is faster for NR2A than for NR2B. We interpret these data to suggest that conformational changes controlled by glutamate binding have a lower activation energy for NR2A- than for NR2B-containing receptors. The difference in these pre-gating steps has a dramatic effect on NR2A and NR2B temporal signalling properties, with important implications for synaptic transmission.

Methods

HEK293 cells were maintained and transiently transfected using the calcium phosphate method for 4–8 h with NR1–1a (GenBank U11418, U08261; pCIneo vector; hereafter NR1), either NR2A (D13211; pCIneo) or NR2B (U11419; pCDNAIamp), and green fluorescent protein (GFP) at a ratio of 1 : 2 : 0.5 as previously described (Banke & Traynelis, 2003). Currents from outside-out patches, held at potentials (V_m) ranging between −60 and −80 mV, were recorded using an Axopatch 200A or 200B amplifier (Axon Instruments) and were digitized with Pclamp8 software. Single-channel data for both concentration jumps and steady-state recording were filtered at 5 kHz using an 8-pole Bessel filter (−3 dB, Frequency Devices) and digitized at 13–40 kHz. Steady-state currents were typically recorded for 5 min. Macroscopic currents were filtered at 2 kHz and digitized at 20 kHz. The extracellular solution for NR2A experiments consisted of (mM): NaCl 150, Hepes 10, $CaCl_2$ 0.5, KCl 3 and EDTA 0.01, with 50 μM glycine and 1 mM glutamate unless otherwise noted (pH 7.3, 23°C). The extracellular solution for NR2B experiments consisted of (mM): NaCl 150, Hepes 10, $CaCl_2$ 0.5, KCl 3 and Ca-EDTA 0.2, with 20 μM glycine and 1 mM glutamate unless otherwise noted (pH 7.4, 23°C). For most experiments, the agonist-containing extracellular solution was made from ultra-pure salts with a Mg^{2+} concentration of < 0.2 μM measured using inductively coupled plasma mass spectroscopy by the Laboratory for Environmental Analysis, University of Georgia. Channel data recorded with normal salts were included in the final analysis as measured Mg^{2+} concentration was < 1 μM and the mean channel open time was not significantly different in paired comparisons of normal and ultra-pure salts in the same patches expressing NR1/NR2A ($P > 0.05$, $n = 6$). The internal solution consisted of (mM): caesium gluconate 110, $CsCl_2$ 30, Hepes 5, NaCl 4, $CaCl_2$ 0.5, $MgCl_2$ 2, BAPTA 5, Na_2ATP 2 and Na_2GTP 0.3 (pH 7.35). Rapid solution exchange was achieved with a two-barrel theta glass pipette controlled by a piezoelectric translator (Burliegh); junction currents were used to estimate speed of solution exchange after recordings. Exchange times for 10–90% solution were typically ∼1 ms, or 7- to 12-fold faster than the current rise times in response to a saturating agonist concentration. Brief pulses for the single-channel experiments had a half-width of 6–8 ms for NR1/NR2A and 3–5 ms for NR1/NR2B. Brief pulses for the macroscopic experiments had a half-width of 15–20 ms for NR1/NR2A and 6–8 ms for NR1/NR2B.

Outside-out patches were assumed to contain a single channel when we could detect no double openings in response to more than 50 brief agonist applications or during at least 2 min of continuous recording in the presence of agonist. In addition, the homogeneous peak open probability and observation that numerous other patches contained zero or two active channels further suggest our recordings contain only a single active channel. Single-channel analysis was performed using QUB software (www.qub.buffalo.edu) to idealize records and fit kinetic models to idealized single-channel data. For histogram fitting, the data were divided into uniform segments (0.5–10 s for NR2A and 1–10 s for NR2B) and any segment with simultaneous multiple channel openings was discarded. Records were idealized with the segmentation k-means algorithm (Qin, 2004).

Dwell time distributions were fit to multiple exponential kinetic components using ChanneLab (www.synaptosoft.com). For maximum interval likelihood (MIL; Qin *et al.* 1997) fitting data were idealized and segmented with a critical shut duration (Tcrit) calculated that minimized the total number of misclassified events (Jackson *et al.* 1983; Colquhoun & Sigworth, 1995; EKDIST provided by David Colquhoun,

University College, London). Idealized activations were then fitted to hidden Markov models using the maximum interval likelihood method. A subset of six NR1/NR2B-containing one-channel patches activated by glutamate described by Banke & Traynelis (2003) were re-analysed here, and the results included for comparison with parallel experiments with NR2A. For macroscopic currents, macroscopic response waveforms obtained in outside-out patches were normalized and averaged among patches. The average macroscopic glutamate response waveform was then normalized to the measured open probability determined in one-channel patches. Hidden Markov models were simultaneously fitted (ChanneLab) to multiple macroscopic waveforms obtained for both short and long pulses of agonist and high and low concentrations of agonist. Simulated responses to synaptic waveforms of glutamate were generated using Channelab at 50 kHz.

ANOVA with Tukey's *post hoc* test was performed for multiple comparisons and Student's *t* test was used for paired comparisons. Data are expressed as means ± S.E.M.

Results

Activation of NR1/NR2A and NR1/NR2B receptors by brief glutamate application

Recombinant NR1/NR2A or NR1/NR2B receptor function was evaluated by applying a brief (3–8 ms) synaptic-like pulse of 1 mM glutamate in the continued presence of 50 μM glycine to outside-out patches excised from transiently transfected HEK293 cells (Fig. 1). Under some conditions, NMDA receptors display multiple conductance states that probably reflect fluctuations in the energetics of ion permeation through the pore (Cull-Candy & Wyllie, 1991; Premkumar

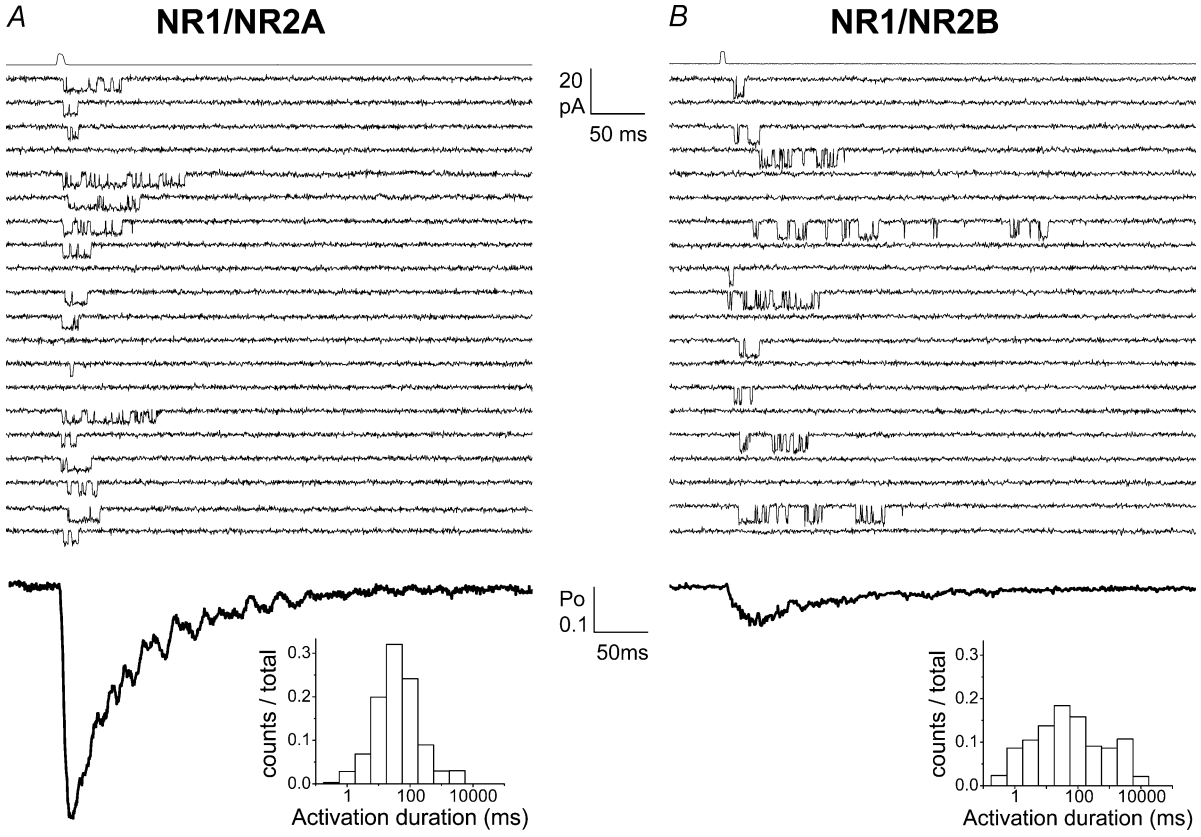

Figure 1. Activation of NR1/NR2A or NR1/NR2B channels in outside-out patches in response to a synaptic-like brief pulse of saturating glutamate
A and *B*, patches with only a single active NR1/NR2A or NR1/NR2B channel were exposed to a brief (3–8 ms) pulse of 1 mM glutamate in the continued presence of 50 μM glycine. The tip current used to determine the time course of solution exchange is plotted on the top trace. Twenty representative current responses from one patch are displayed for NR1/NR2A or NR1/NR2B channels (resampled at 2.5 kHz and filtered at 1 kHz for display; $V = -80$ mV for NR1/NR2A, -100 mV for NR1/NR2B). The mean current response for each patch was normalized to the unitary channel current to convert the waveform to an absolute open probability. This open probability waveform was averaged among six patches and the resulting composite open probability waveform is displayed below the individual current traces. The distribution of activation durations, defined as the total time between and including the first and last channel opening, is shown as an inset adjacent to the open probability mean waveform.

Table 1. The open probability of single activations in response to a brief pulse of glutamate

	NR1/NR2A	NR1/NR2B
Probability of activation	0.802 ± 0.018	0.558 ± 0.061
Open probability within an activation	0.670 ± 0.044	0.330 ± 0.040
Peak open probability	0.496 ± 0.030	0.119 ± 0.012

Values are mean ± S.E.M. for six patches for each subunit combination. Probability of activation is the fraction of sweeps with at least one channel opening following agonist application. Open probability within an activation is the fraction of time open during the activation. The peak open probability is calculated for each patch by normalizing the peak of the mean current waveform to the unitary current.

et al. 1997). However, in the presence of a relatively low (0.5 mM) Ca^{2+} concentration, we observe one predominant conductance level (NR1/NR2A, 62.3 ± 1.3 pS; NR1/NR2B, 67.8 ± 3.7 pS, $n = 6$ for both). Only patches that contained one active channel were analysed (see Methods). This experimental design of applying a brief pulse of a maximally effective concentration of glutamate to a patch expressing only a single active channel has several advantages compared to the analysis of macroscopic currents or the analysis of unitary currents with multiple active channels in the patch. First, it is possible to measure directly the probability that the channel will open following a single agonist binding event. If we assume application of 1 mM glutamate ($> 100 \times EC_{50}$) always leads to receptor binding, then the probability that an agonist-bound receptor will open at least once can be calculated by determining the fraction of responses that contain at least one opening after glutamate application. Second, normalizing the mean current response to the amplitude of the unitary (single-channel) current gives a direct measurement of the magnitude and time course of channel open probability following agonist binding. Third, the durations of defined single activations can be determined unequivocally without the complication of agonist rebinding, allowing direct measurement of both activation duration and open probability within an individual activation.

Representative current traces from one patch are shown for NR1/NR2A or NR1/NR2B in Fig. 1. The mean open probability waveform averaged across six patches is displayed below the individual current traces for both NR1/NR2A and NR1/NR2B. A number of differences can be seen within the raw current traces. For example, NR1/NR2A receptors are more likely to open, while activations of NR1/NR2B are of longer duration than NR1/NR2A. Activation parameters summarized in Table 1 highlight several functional distinctions between NR1/NR2A and NR1/NR2B. Of the three different measures of channel open probability made, $P_{\text{activation}}$ refers to the fraction of sweeps which have at least one channel opening following application of a supra-maximal concentration of agonist. The peak open probability, $P_{\text{o,peak}}$, was calculated by dividing the mean current waveform for each patch by the unitary single-channel current and determining the peak of this waveform. The open probability within an activation, $P_{\text{o,within activation}}$, is defined for each sweep as the total time spent in the open state as a fraction of the activation duration. For all three measures of open probability, NR1/NR2A receptors had a significantly higher value than NR1/NR2B receptors. NR1/NR2A receptors were more likely to activate, showed a higher peak open probability, and had a greater open probability within an activation. We also determined the distribution of activation durations for both NR1/NR2A and NR1/NR2B (inset in Fig. 1*A* and *B*). NR1/NR2B receptors had a broader distribution of activation durations than NR1/NR2A and on average the activation duration was longer for NR1/NR2B than NR1/NR2A, consistent with the slower deactivation time course for NR1/NR2B than NR1/NR2A (Vicini *et al.* 1998; see also Fig. 5*B* and Table 3).

Activation of NR1/NR2A and NR1/NR2B receptors at steady state

Steady-state recordings of NMDA receptor activity in outside-out patches in the presence of saturating concentrations of glutamate and glycine contained many more openings in response to agonist than our brief pulse experiments, and thus provide a valuable complement to that data. The greater number of channel openings per patch in steady state *versus* the brief jump data allowed us to fit hidden Markov models to data from individual patches to evaluate putative gating mechanisms (see below). One example of a patch with NR1/NR2A receptors recorded under steady-state conditions is shown in Fig. 2*A* (digitized at 40 kHz and filtered at 5 kHz). Current data were idealized and the distribution of shut time durations is plotted in Fig. 2*B* (same patch shown in Fig. 2*A*). For comparison, the pooled shut time distribution from six patches for activations following a brief glutamate pulse is shown in Fig. 2*C*. Shut-time distributions from steady-state recordings of NR2A showed a complex bursting behaviour similar to activations elicited by brief agonist application (Fig. 2*B* and *C*). Similar to brief jumps, the steady-state channel shut-time distributions show one very brief component (0.1 ms) and two main components with time constants of 0.55 ± 0.05 ms (area, $29.2 \pm 3.2\%$) and 3.63 ± 0.37 ms (area, $39.3 \pm 2.2\%$; $n = 7$). Steady-state recordings do exhibit long desensitized periods of inactivity in the continued presence of agonist similar to

those occasionally observed in activations following brief glutamate application.

A parallel set of recordings was performed for NR1/NR2B receptors (Fig. 3). Figure 3*A* shows an example of NR1/NR2B channel activity recorded at steady state. Current data were idealized and the distribution of shut-time durations is plotted in Fig. 3*B* (same patch shown in Fig. 3*A*). For comparison, the pooled shut-time distribution from six patches for activations following a brief glutamate pulse is shown in Fig. 3*C*. Shut-time distributions from steady-state recordings of NR1/NR2B showed a complex behaviour similar to activations elicited by brief agonist application (Fig. 2*B* and *C*). Similar to brief jumps, the steady-state channel shut-time distributions show one very brief component (0.1 ms) and two main components with time constants of 1.04 ± 0.25 ms (area, $21.2 \pm 1.4\%$) and 20.6 ± 3.3 ms (area, $36.6 \pm 6.5\%$; $n = 6$). The mean channel open time was similar for NR1/NR2A and NR1/NR2B receptors (NR1/NR2A, 3.72 ± 0.39 ms, $n = 7$; NR1/NR2B, 3.33 ± 0.47 ms, $n = 9$).

Comparison of NR1/NR2A and NR1/NR2B gating mechanisms

A number of previous studies have argued convincingly that at least two pre-gating kinetically distinct conformation changes are required before NMDA receptors can open (Gibb & Colquhoun, 1991; Banke & Traynelis, 2003; Popescu & Auerbach, 2003; Popescu *et al.* 2004). We used hidden Markov modelling of our single-channel data to explore whether differences exist between rates of motion for these hypothetical conformational changes that precede pore dilation for

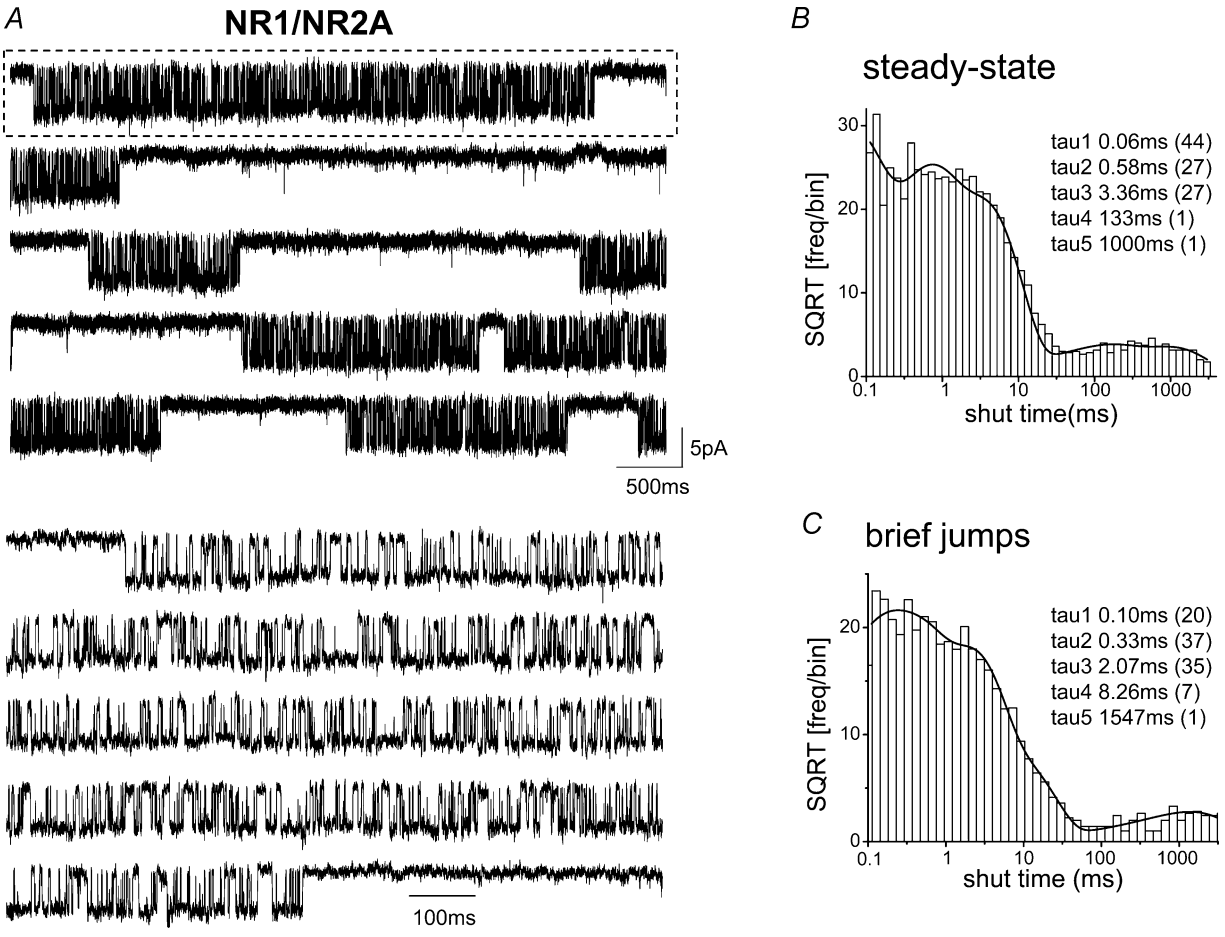

Figure 2. Steady-state NR1/NR2A currents in outside-out patches
A, steady-state recording of a patch with a single NR1/NR2A channel displayed on two different time scales ($V_m = -80$ mV, digitized at 40 kHz, filtered at 5 kHz). The box in the top trace highlights the region shown in detail in the bottom trace. The shut time duration histogram (*B*) of the same patch in (*A*) shows multiple exponential components described the histogram. The time constants are given in the inset with the percentage area for each component in parentheses. *C*, the distribution of shut durations pooled from six patches following a brief jump into saturating glutamate (see Figure 1) is plotted for comparison with the steady-state data in *B*.

NR1/NR2A and NR1/NR2B receptors. Patches of high quality and sufficient number of events were selected for analysis for NR1/NR2A or NR1/NR2B receptor activations. Data were analysed by subdividing records on the basis of a critical shut time (30 ms for NR1/NR2A, 100 ms for NR1/NR2B) that was calculated to separate openings occurring within the same activation from openings within two different activations (see Methods). Table 2 compares the mean (± S.E.M.) rate constants for three different representations of NR1/NR2A or NR1/NR2B receptor activation (Fig. 4). Because the recordings were performed in the continuous presence of a saturating concentration of both glutamate and glycine, no explicit binding steps are included and full occupancy of ligand binding sites is assumed.

Scheme 1 is adapted from Banke & Traynelis (2003) and postulates the existence of independent NR1 and NR2 subunit transitions, both of which must occur, before the channel pore can open. These two conformational changes (a relatively fast transition 'f', and a slow transition 's') can occur in either order. The original interpretation of the results obtained with this model was that the faster rate reflects NR1 conformational changes and the slower rate reflects NR2 conformational changes based on sensitivity of the kinetics to partial agonists acting at the glycine or glutamate site, respectively (Banke & Traynelis, 2003). Scheme 1 provides a reasonable fit to the sequence of steady-state single-channel openings and closings. The only rate constant differing significantly between NR1/NR2A and NR1/NR2B is k_{s+}, the forward rate previously suggested to largely reflect the slower activation step, with NR1/NR2A having a faster activation rate than NR1/NR2B (Table 2). The observation that only the slow rate differs between NR1/NR2A and NR1/NR2B containing receptors supports the conceptual model that this particular rate reflects actions within NR2, since only

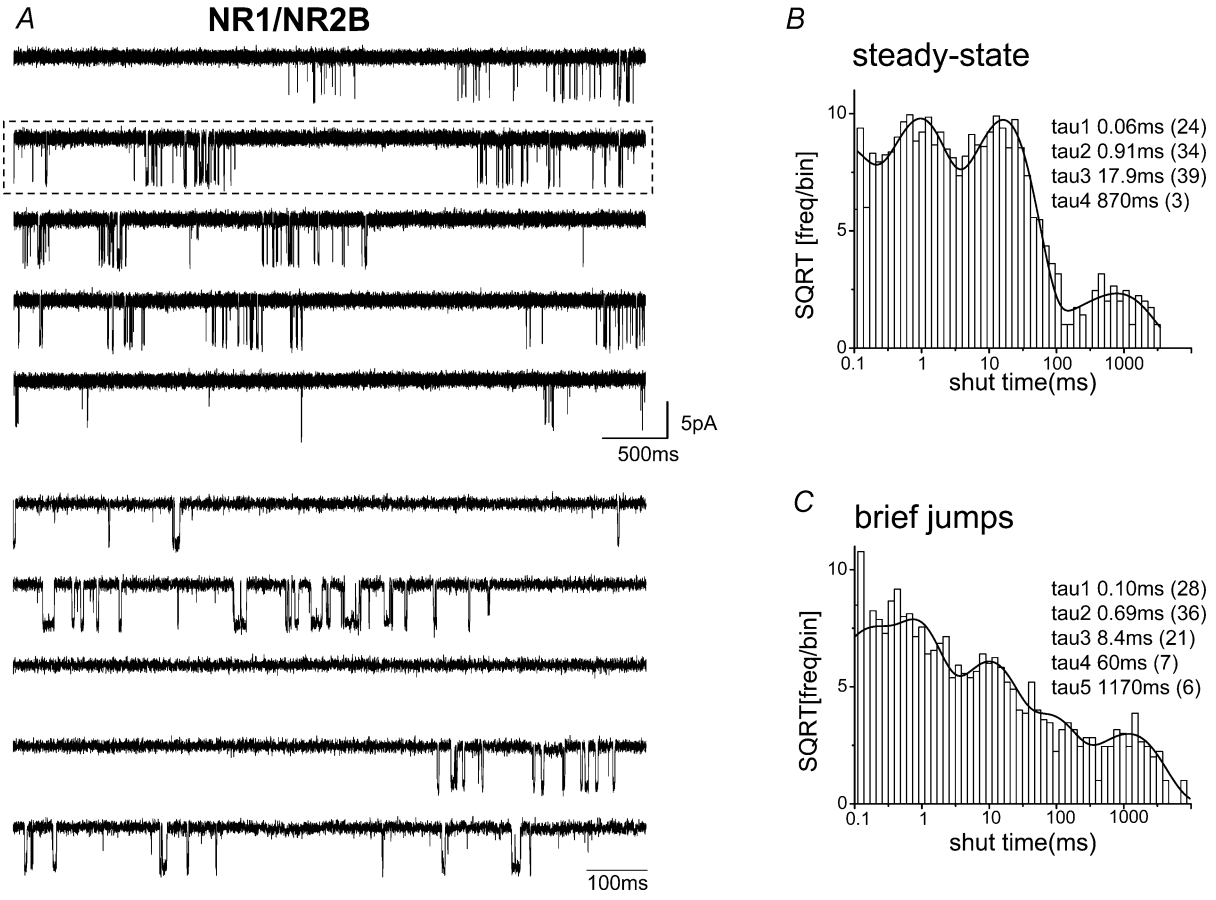

Figure 3. Steady-state NR1/NR2B currents in outside-out patches
A, steady-state recording of a patch with a single NR1/NR2B channel displayed on two different time scales shows bursting behaviour ($V_m = -100$ mV, digitized at 40 kHz, filtered at 5 kHz). The box in the top trace highlights the region shown in detail in the bottom trace. *B*, the shut-time duration histogram of the same patch as in *A* shows multiple exponential components, with longer time constants reflecting recovery from desensitization. The time constants are given in the inset with the percentage area for each component in parentheses. *C*, the distribution of shut durations pooled from six patches following a brief jump into saturating glutamate (see Figure 1) is plotted for comparison with the steady-state data in *B*.

the subunit (NR2) differs between the hetero-dimeric NR1/NR2A and NR1/NR2B complexes.

Schemes 2 and 3 are alternative hypotheses in which there are multiple conformational changes preceding opening of the channel pore that are constrained to be sequential. For Scheme 2 the forward activation rates for the first step k_{1+} is faster for NR1/NR2A than for NR1/NR2B. The quality of the fits to both Schemes 1 and 2 were similar as quantified by the log likelihood per event (Scheme 1, 4.33 ± 0.11; Scheme 2, 4.34 ± 0.10, $n = 10$) and both models have an equal number of parameters. Therefore we cannot distinguish between these two models on statistical criteria. Both Schemes 1 and 2 are an oversimplification in that they predict only one open state, whereas the data show at least two distinct kinetic components to the open dwell time distribution (note the briefest openings are poorly fit by Scheme 1). Scheme 3 is a sequential scheme, similar to that proposed by Popescu *et al.* (2004), which contains one additional closed and one additional open state compared to Schemes 1 and 2. This Scheme possesses more free parameters and provides a better description of the dwell-time distributions. The interpretation of the fits to Scheme 3 is conceptually similar to Schemes 1 and 2 in that the forward rate for the first or slowest of the sequential conformational changes is faster for NR1/NR2A than for NR1/NR2B. Results from evaluation of all three of these models suggest that multiple pre-gating steps are needed for both receptors, and that NR1/NR2A undergoes one of these conformational changes more rapidly than NR1/NR2B. Consistent with this hypothesis, the cumulative first latency histograms and rise time for the mean waveform from one-channel patches confirm the more rapid activation of NR1/NR2A than NR1/NR2B (Fig. 5; see also rise times of macroscopic currents in Table 3).

Agonist binding, activation and desensitization of NR1/NR2A and NR1/NR2B receptors

In order to evaluate the effects that subunit-specific gating properties might have at synaptic receptors, we fitted macroscopic responses with models that incorporated our information about gating and also included explicit binding and desensitization rates. Macroscopic currents in outside-out patches were recorded in response to rapid application of glutamate in the continued presence of 50 μM glycine. Three sets of responses were generated for each receptor: (1) a long pulse of high agonist concentration; (2) a brief pulse of high agonist concentration; and (3) a long pulse of low agonist concentration (Fig. 6*A*). Responses for each condition were normalized and averaged across patches (Fig. 6*B*). Kinetic parameters describing the time course of macroscopic currents are given in Table 3*A*. Two exponential components were required to fit the desensitization profile of responses recorded in the continued presence of glutamate or the deactivation following a brief pulse of glutamate. The amplitude of the responses to prolonged application of the high (1 mM)

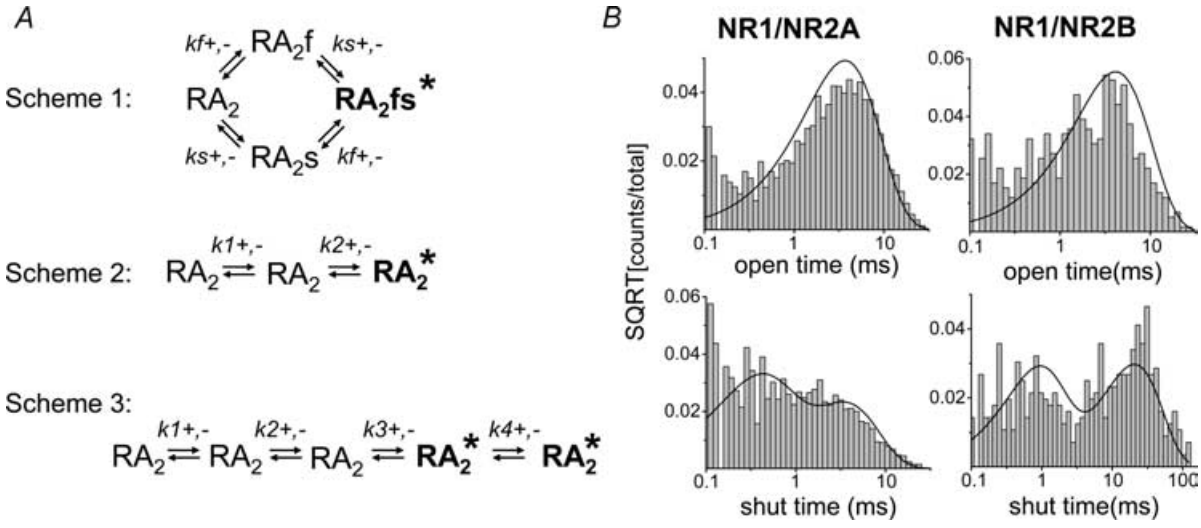

Figure 4. Maximum interval likelihood fitting of steady-state activations of NR1/NR2A or NR1/NR2B
A, kinetic models are depicted for each scheme with open-channel states in bold with a star. Scheme 1 postulates two independent pre-gating steps. Scheme 2 postulates two sequential pre-gating steps. Scheme 3 is an extension of Scheme 2 with an additional open and shut state to account for the briefest component of the dwell-time distributions. *B*, steady-state currents were idealized and fitted to Scheme 1. Bar graphs show dwell-time distribution histograms for one example patch for each subunit combination and solid lines show probability density functions predicted by model fits. Rate constant results from fits to all three models are given in Table 2.

Table 2. Hidden Markov maximum interval likelihood fitting of steady-state currents

	NR1/NR2A		NR1/NR2B		%	*t* test
rate	s^{-1}	± S.E.M.	s^{-1}	± S.E.M.	difference	*P* value
Scheme 1						
k_{s+}	230	26	48	4	379	< 0.001
k_{s-}	178	26	230	29	−23	0.21
k_{f+}	3140	183	2836	440	11	0.53
k_{f-}	174	4	175	31	−1	0.98
Scheme 2						
k_{1+}	434	30	131	15	231	< 0.001
k_{1-}	1405	114	1682	199	−16	0.25
k_{2+}	1755	160	1311	294	34	0.21
k_{2-}	351	27	404	49	−13	0.34
Scheme 3						
k_{1+}	356	24	151	36	136	<0.001
k_{1-}	201	25	350	118	−43	0.25
k_{2+}	944	177	543	129	74	0.08
k_{2-}	2758	717	2833	463	−3	0.93
k_{3+}	2849	738	2111	630	35	0.46
k_{3-}	2835	430	3810	1052	−26	0.41
k_{4+}	4979	842	3935	617	27	0.33
k_{4-}	970	124	852	90	14	0.45

Values are mean ± S.E.M. for 10 patches for NR1/NR2A and 11 patches for NR1/NR2B. Kinetic models for each scheme are depicted in Fig. 4*A*. ' + ' indicates the forward rate and '–' indicates the reverse rate. % difference is relative to the rate for the NR2B subunit. %diff = 100 × (2A–2B)/2B. The log likelihood for global fits of each model to pooled data from all patches are: NR1/NR2A scheme1 742419.56, scheme2 742411.05, scheme3 753794.39; NR1/NR2B scheme1 216209.79, scheme2 216211.42, scheme3 222377.81.

agonist concentration response were constrained to match the empirically determined peak open probability (Fig. 1 and Table 1), and other responses were scaled according to their mean relative amplitudes in the same patches. All three curves for each agonist were simultaneously fitted with Scheme 4, an extension of the independent subunit activation model fitted to the single channel data above (Scheme 1). In Scheme 4 there are two independent glutamate binding steps (explicit glycine steps are omitted as all recordings were performed in the presence of a saturating concentration of glycine at all times) and two desensitized states (reflecting the double exponential nature of the desensitization time course). The gating rates were fixed to those determined from single-channel analysis and the only free parameters in these fits were the binding and desensitization steps. A least-squares criterion was used to find a set of rate constants which minimized the difference between experimental and simulated waveforms. The resulting fits of the data to this Scheme are shown in Fig. 6*B*. Table 3*B* summarizes the results from fitting Scheme 4 to macroscopic data for both NR1/NR2A and NR1/NR2B, and confirms that these conceptual models can predict responses to synaptic-like stimuli with the correct time course and the correct open probability.

Subunit-specific gating controls synaptic signalling by NR1/NR2A and NR1/NR2B receptors

The models described in Table 3*B* and Fig. 6 predict not only different open probability and response time course for NR1/NR2A and NR1/NR2B receptors, but also different concentration dependence. For example, Scheme 4 predicts an EC_{50} value for the peak response of 6.1 μM (Hill slope or n_H of 1.7) for NR1/NR2A and 7.8 μM (n_H of 1.2) for NR1/NR2B receptors. The EC_{50} values for the steady-state response, estimated as the plateau current in response to 5-s application of glutamate, were predicted to be 2.6 μM (n_H of 1.6) and 1.2 μM (n_H of 1.9) for NR1/NR2A and NR1/NR2B, respectively. In order to evaluate how these differences in channel gating and response properties between NR2 subunits can affect NMDA receptor-mediated synaptic signalling, we simulated responses to synaptic glutamate waveforms using the results of the fitting to Scheme 4. The simulated synaptic glutamate waveform had a peak concentration of 1.1 mM and decayed with an exponential time constant of 1.2 ms (Clements *et al.* 1992). Figure 7 illustrates the current response of 20 NR1/NR2A or NR1/NR2B channels, held at a membrane potential of −60 mV, to a single synaptic pulse of glutamate. While these simulations are of voltage-clamped receptors in the

absence of magnesium block, we feel that they are a useful starting point to evaluate how the differences in channel kinetics we have described here would give rise to different synaptic responses. We quantified the charge transfer (Q) by integrating the current response (measuring the area under the current trace) at different time points after the stimulus. The time course for total charge transfer from a single synaptic stimulus is illustrated in the inset in Fig. 7. Activation of NR1/NR2A receptors results in a relatively fast charge transfer, reaching 85% of the total within the first 100 ms. By contrast, the relatively prolonged activation for NR1/NR2B results in a slower accumulation of charge, exceeding 50% of total charge only after 1 s. The total charge transfer by a synaptic activation is approximately 2-fold greater for NR1/NR2B than NR1/NR2A. This occurs because the deactivation of NR1/NR2B receptors is so much slower than NR1/NR2A receptors that it more than compensates for the lower open probability for NR1/NR2B.

NR1/NR2A and NR1/NR2B receptors differ in their rates of deactivation and desensitization, as well as their recovery from desensitization. Given the influence that NR2 subunits exert on the temporal signalling profile of NMDA receptors, we evaluated the frequency dependence of charge transfer using our models of NR2A- and NR2B-containing receptors. Our ability to accurately model both the time course and peak open probability allows us to compare the predicted response for receptors with each subunit to the same synaptic glutamate concentration profile. We used trains of six pulses varying in frequency between 0.25 and 50 Hz. Figure 8*A* illustrates the frequency dependence of charge transfer for NR2A- and NR2B-containing receptors. At low frequencies, NR1/NR2B receptors retain their ability to pass more current than NR1/NR2A. However, at higher frequencies, NR1/NR2A receptors become equally effective as NR1/NR2B at passing current for our six-pulse stimulus protocol. In order to further explore the differential response to high-frequency stimulation, we examined the simulated responses of NR1/NR2A and NR1/NR2B receptors to different duration trains of high-frequency (100 Hz) tetanic stimuli (Fig. 8*B*). Stimulation of NR1/NR2A receptors by a 100-Hz train of synaptic glutamate pulses resulted in significantly more charge transfer than for NR1/NR2B provided the duration of the stimulus train exceeded 100 ms. This was largely due to a difference in the glutamate unbinding rate, with NR2A releasing agonist 30-fold faster than NR2B, which reduces the degree of desensitization for NR1/NR2A compared to NR1/NR2B in response to a single synaptic stimulus.

We subsequently examined whether the predicted differential charge transfer and differential frequency dependence for NR1/NR2A and NR1/NR2B receptors will also apply to synaptic glutamate time courses other than that tested above (e.g. Barbour, 2001). We examined peak glutamate concentrations between 0.1 and 10 mM and time course of glutamate removal approximated as an exponential function with time constants between 0.1 and 10 ms. NR1/NR2A receptors produced a 2-fold greater charge transfer than NR1/NR2B receptors in response to high-frequency tetany for all synaptic concentrations and time courses tested. We also repeated each of the simulations described in Figs 7 and 8 for differing synaptic profiles. The differential charge transfer between NR1/NR2A and NR1/NR2B was similar for synaptic glutamate time courses that produced full but brief receptor activation. For example, when the glutamate time constant was 10 ms, the difference between NR2A and NR2B were less pronounced than for a time constant of 1 ms. When the synaptic glutamate concentrations decayed with a time constant of 0.1 ms, only the highest glutamate concentration (10 mM) showed a similar differential charge-transfer profile between NR1/NR2A and NR1/NR2B to that shown in Fig. 7. In contrast, for a glutamate time constant of 1 ms, the

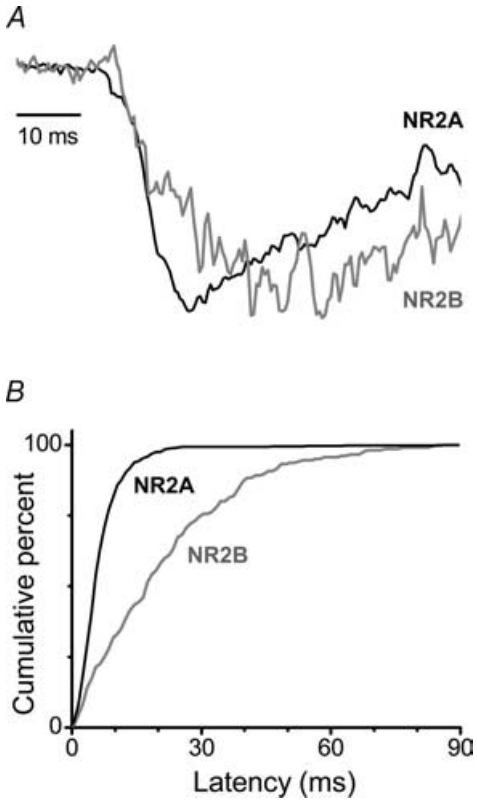

Figure 5. Activation rate for NR1/NR2A and NR1/NR2B
A, the rising phase of the ensemble average from one-channel patches activated by brief concentration jump to maximally effective concentration of glutamate (1 mM). Average waveforms were normalized and superimposed; $n = 6$ patches for both NR1/NR2A and NR1/NR2B. *B*, cumulative first latency histogram was constructed for three patches for both NR1/NR2A (556 events) and NR1/NR2B (205 events). The cumulative distribution for the first 90 ms was normalized to 100%, and shows that NR2A activates faster than NR2B ($P < 0.001$; Kolmogorov-Smirnov).

charge transfer ratio of NR2A:NR2B was independent of the glutamate concentration in the range of 1–10 mM. This effect was mirrored in the simulations evaluating the effects of frequency on charge transfer. These data suggest that the differential response of NR2A- and NR2B-containing receptors to high-frequency stimulation is independent of synaptic glutamate response waveform, whereas the frequency dependence of charge transfer for low-frequency LTD-like stimuli require full receptor activation and brief glutamate pulses.

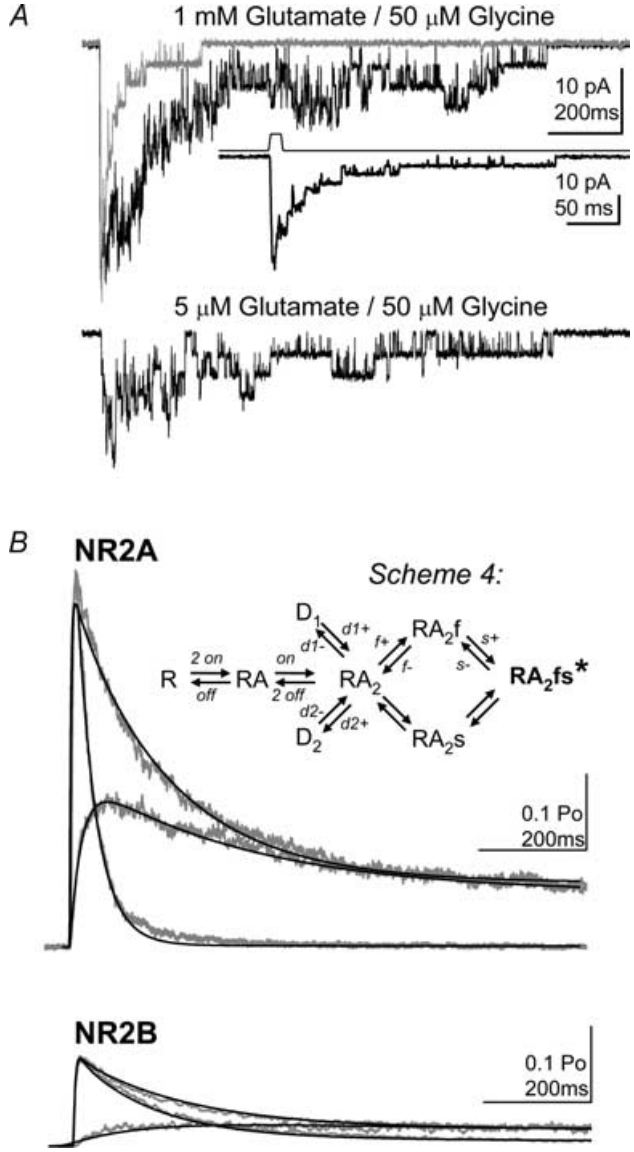

Figure 6. Fitting of macroscopic currents to determine agonist binding and desensitization rates
A, macroscopic currents for curve fitting were recorded in outside-out patches excised from HEK293 cells expressing NR1/NR2A ($V_m = -60$ mV). One example sweep is shown for each of the three protocols: 1 mM glutamate brief pulse; 1 mM glutamate long pulse; and 5 μM glutamate long pulse. The inset shows the brief 1 mM glutamate response on an expanded time scale with the junction current used to determine the time course of solution exchange. *B*, the mean waveform for each protocol is shown for both NR1/NR2A and NR1/NR2B (grey, $n = 11$ NR1/NR2A, $n = 17$ NR1/NR2B). For NR2B the three protocols are: 1 mM glutamate brief pulse; 1 mM glutamate long pulse; and 3 μM glutamate long pulse. Fits to Scheme 4 are in black and raw data in grey are mean normalized currents. In the model there are two different desensitized states which are accessible from the fully liganded state (RA_2 in Scheme 4). Kinetic parameters and fitting results are given in Table 3.

Discussion

There are four main findings of this study. First, receptors containing the NR2A subunit have a higher open probability than those containing the NR2B subunit, quantified as either the probability of activation, the peak open probability or the open probability within an activation. Second, following agonist binding there are multiple pre-gating conformational transitions prior to channel opening, with at least one of these changes being faster for NR1/NR2A receptors than for NR1/NR2B receptors. The change in this rate accounts for differences in open probability and current rise times. Third, a simple model incorporating two pre-gating activation steps can account for NR1/NR2A or NR1/NR2B currents in response to rapid agonist application over a range of agonist concentrations and durations, as well as correctly predict the peak open probability measured directly from single channels. These models also predict the main features of single-channel records. Finally, these

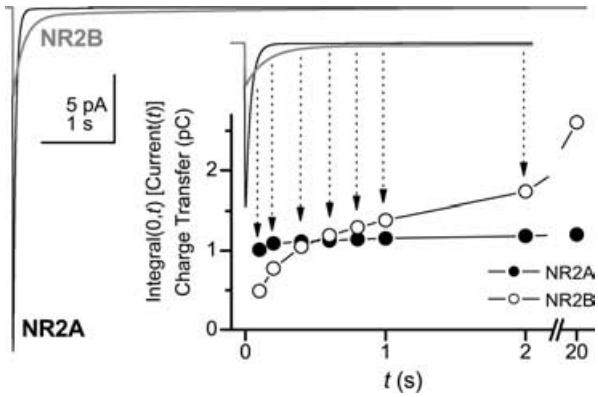

Figure 7. Subunit-specific gating controls NR2 subunit-dependent signalling properties
Models using Scheme 4 with the rates listed in Table 3 were used to simulate NR1/NR2A or NR1/NR2B response to synaptic inputs. A peak glutamate concentration of 1.1 mM with an exponential decay time constant of 1.2 ms was used to drive simulations (Clements *et al.* 1992). The response to a single synaptic pulse of glutamate is simulated for 20 channels at −60 mV under voltage clamp (50 pS conductance, with a reversal potential of 0 mV). Inset, the accumulated charge transfer for NR2A- and NR2B-containing receptors is calculated at varying time points of the current response following stimulation. The current response is plotted on the same time scale with arrows indicating the corresponding time point between the current response and the accumulated charge transfer. Calcium entry is proportional to charge transfer as the relative permeability for calcium is the same for NR1/NR2A and NR1/NR2B (Schneggenburger, 1996).

NR2 subunit-dependent gating differences cause dramatic differences in both the timing of charge transfer as well as the response of these receptor-channels over a range of stimulation frequencies. Thus, the ability of NR2 subunit to control open probability and temporal signalling may influence the differential contribution of NR2A- and NR2B-containing receptors to various forms of synaptic plasticity.

Functional implications of activation of NMDA receptors

It has previously been shown for AMPA receptors that partial agonists induce only partial closure of the agonist binding S1S2 domain (Armstrong & Gouaux, 2000). AMPA receptors exhibit multiple conductance levels and it has been hypothesized that each subunit can gate independently and make an incremental contribution to ion permeation such that channel conductance depends on the number of agonist-binding sites occupied (Rosenmund *et al.* 1998; Smith & Howe, 2000). A compelling convergence of structure and function was achieved by Jin *et al.* 2003) who demonstrated that the degree of domain closure induced by partial agonists correlates directly with the functional efficacy for the coupling of agonist binding to channel gating. How this finding relates to NMDA receptor function is unclear, as the properties of channel gating for NMDA receptors differ significantly from AMPA receptors (reviewed by Erreger *et al.* 2004). For example, NMDA receptors must be fully liganded to open and there is evidence for multiple conformational changes required to transduce agonist binding into channel gating (Popescu & Auerbach, 2003; Banke & Traynelis, 2003; Popescu *et al.* 2004; commentary by Magleby, 2004; Gibb, 2004). Our finding that exchange of the NR2 subunit alters a rate constant that has been hypothesized to be an NR2-controlled conformational change and which precedes channel opening (Banke & Traynelis, 2003) is consistent with individual subunits undergoing independent activating conformational transitions. Precedent exists for this idea, which has been proposed not only for glutamate receptors (Jin *et al.* 2003; Banke & Traynelis, 2003) but also for both cyclic nucleotide-gated channels and shaker potassium channels (reviewed by Karpen & Ruiz, 2002).

The different efficiency by which NR1/NR2A and NR1/NR2B receptors undergo a pre-gating conformational change will also influence open probability. Previous measurements of the subunit dependence of open probability relying on the blocking properties of the open channel blocker MK-801 (Jahr, 1992) predicted that NR1/NR2A receptors have a 2- to 5-fold higher open probability than NR1/NR2B receptors (Chen *et al.* 1999). Here we report, using direct measurements of experimentally defined individual activations of a single receptor-channel, the peak open probability of NR2A- and NR2B-containing receptors. NR1/NR2A channels exposed to a synaptic-like (brief, high concentration) glutamate stimulus exhibited a 4-fold greater peak open probability than NR1/NR2B (0.50 for NR1/NR2A *versus* 0.12 for NR1/NR2B). Additionally, we find the probability that a fully liganded receptor-channel will open at least once, which we refer to as $P_{\text{activation}}$, is 0.80 for NR1/NR2A and 0.56 for NR1/NR2B. This measured value for NR1/NR2A is slightly higher than

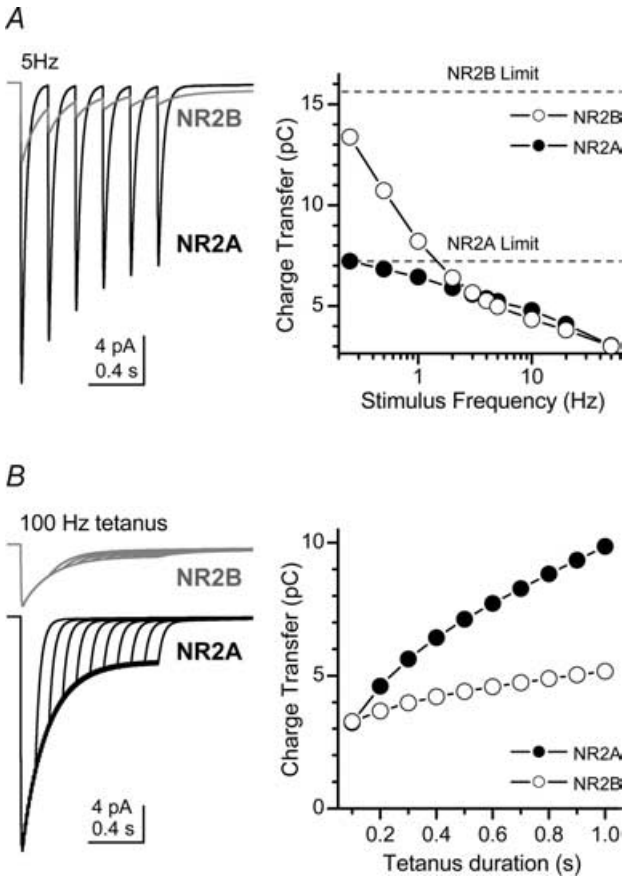

Figure 8. NR1/NR2A and NR1/NR2B show distinct frequency dependence of signalling
A, NR1/NR2A and NRI/NR2B receptor responses were simulated in response to trains of six synaptic pulses at 5 Hz (left panel). There is a clear difference in the amplitude of the current response to each pulse between NR1/NR2A and NR1/NR2B receptors. The right panel summarizes the total charge transfer (total area under the current curve for the entire train of six synaptic pulses) at different frequencies. The low-frequency limit of the charge transfer was calculated as six times the charge transfer to a single response, and is shown for both NR1/NR2A and NR1/NR2B (broken line). Low-frequency stimulation allows higher charge transfer, and therefore calcium entry, through NR1/NR2B receptors, whereas moderately higher stimulus frequencies lead to similar levels of overall charge transfer for the two subunits. *B*, summary of charge transfer for a 100-Hz tetanic stimulus train of a varying duration. High-frequency stimulation for $>$ 100 ms produces greater charge transfer, and therefore calcium entry, through NR1/NR2A than NR1/NR2B receptors.

Table 3. Kinetic parameters and least-squares fitting of macroscopic data

A Kinetic parameters	Units	NR1/NR2A	NR1/NR2B	% difference
10–90% rise time	ms	7.4 ± 0.7	11.6 ± 1.2	-36^*
Deactivation	ms	32.1	128	−75
τ_1 (% area)		(94%)	(82%)	
Deactivation	ms	202	799	−75
τ_2 (% area)		(6%)	(18%)	
Desensitization	ms	59.9	142	−58
τ_1 (% area)		(38%)	(85%)	
Desensitization	ms	257	888	−71
τ_2 (% area)		(62%)	(15%)	
B Fitted rate constants	Units	NR1/NR2A	NR1/NR2B	% difference
k_{d1+}	s^{-1}	85.1	550	−85
k_{d1-}	s^{-1}	29.7	81.4	−64
k_{d2+}	s^{-1}	230	112	105
k_{d2-}	s^{-1}	1.01	0.91	11
k_{on}	$\mu M^{-1}\ s^{-1}$	31.6	2.83	1017
k_{off}	s^{-1}	1010	38.1	2551
K_d	μM	32.0	13.5	137

A, 10–90% rise time measurements were made for individual patches ($n = 18$ for NR1/NR2A, $n = 8$ for NR1/NR2B; $^*P < 0.05$). The deactivation or desensitization time course of mean waveforms was fitted to a double exponentially decaying function. *B*, fitting of macroscopic currents (see Fig. 5) to Scheme 4 with k_{f+}, k_{f-}, k_{s+}, k_{s-} fixed to values determined from single-channel data (Fig. 4 and Table 2) was used to determine binding and desensitization constants. $K_d = k_{off}/k_{on}$. Percentage difference is relative to the rate for the NR2B subunit. %diff = 100 × (2A–2B)/2B.

predictions made from simulations by Popescu *et al.* (2004) based on the agonist concentration dependence of single-channel kinetics.

Physiological relevance of pre-gating differences for NR1/NR2A and NR1/NR2B

Expression of NR2 subunits varies both developmentally and anatomically (Sheng *et al.* 1994; Monyer *et al.* 1994). Additionally, some forms of plasticity may be regulated selectively by NR2 subunit composition (Hrabetova *et al.* 2000; Yoshimura *et al.* 2003; Liu *et al.* 2004; Massey *et al.* 2004). For example, LTD can be blocked by NR2B-selective ligands, whereas LTP is insensitive to these compounds. These data were interpreted to suggest that NR2B activation participates in LTD whereas NR2A controls LTP (Liu *et al.* 2004; Massey *et al.* 2004). NR2B subunits are generally expressed preferentially early in development and it has been suggested that slower deactivation time course (longer duration EPSCs) allows for temporal integration of non-synchronous synaptic inputs that may be important for plasticity during neural development (Carmignoto & Vicini, 1992, Flint *et al.* 1997). Figure 7 illustrates the different temporal features of signalling for an equivalent number of NR1/NR2A and NR1/NR2B channels, and highlights how NR2B is more effective in mediating charge transfer following a single synaptic event (or multiple events at low frequency) despite its lower open probability. Because the calcium permeability is similar for NR1/NR2A and NR1/NR2B (Schneggenburger, 1996), the time course for charge transfer is indicative of the time course for calcium entry through NMDA channels. The drastic differences in this profile for calcium entry may underlie the distinct roles suggested for NR1/NR2A and NR1/NR2B in long-term synaptic plasticity. For example, rapid changes in calcium concentration (NR1/NR2A) may activate different cellular signals than a slower calcium signal (NR1/NR2B). Indeed it has been demonstrated that calmodulin can differentially modulate calcium channels in response to rapid local calcium signals or slow diffuse calcium signals (DeMaria *et al.* 2001). Other work suggests both the extent and timing of calcium entry through ion channels may alter gene expression and contribute to synaptic plasticity (Deisseroth *et al.* 2003).

Examination of the frequency dependence of charge transfer highlights an interesting feature of differences in the signalling profiles for NR1/NR2A *versus* NR1/NR2B (Fig. 8). At lower stimulus frequency, such as those typically employed to induce LTD (1 Hz), NR1/NR2B

receptors are more effective at mediating charge transfer and thus Ca^{2+} influx into neurones (Fig. 8*A*). On the other hand, simulation of responses to the type of high-frequency stimulation typically employed to induce LTP (trains of stimulation > 50 Hz for > 100 ms) suggests that NR1/NR2A receptors are more effective at mediating charge transfer and therefore Ca^{2+} influx into neurones (Fig. 8*B*). The differences we observe in intrinsic kinetic properties may explain in part the suggested role for NR2A receptors in LTP and NR2B receptors in LTD (Liu *et al.* 2004; Massey *et al.* 2004). Of course, differential localization or interactions with signalling molecules are among other factors which may contribute to the distinct NR2 subunit roles in long-term plasticity.

Conclusion

Following agonist binding, NMDA receptors must undergo multiple conformational changes prior to channel opening. Our results suggest that at least one of these transitions is regulated by the identity of the NR2 subunit, proceeding more quickly for NR2A than for NR2B. This faster gating explains the higher open probability observed for NR1/NR2A than for NR1/NR2B. However, the activation duration of NR1/NR2B is longer than for NR1/NR2A, resulting in ultimately greater charge transfer and therefore calcium influx. The differences in the time course and frequency dependence of both current and total charge transfer may explain how NR1/NR2A and NR1/NR2B make distinct contributions to synaptic physiology and plasticity.

References

Armstrong N & Gouaux E (2000). Mechanisms for activation and antagonism of an AMPA-sensitive glutamate receptor: crystal structures of the GluR2 ligand binding core. *Neuron* **28**, 165–181.

Banke TG & Traynelis SF (2003). Activation of NR1/NR2B NMDA receptors. *Nat Neurosci* **6**, 144–152.

Barbour B (2001). An evaluation of synaptic independence. *J Neurosci* **20**, 7969–7984.

Brauner-Osborne H, Egebjerg J, Nielsen EO, Madsen U & Krogsgaard-Larsen P (2000). Ligands for glutamate receptors: design and therapeutic prospects. *J Med Chem* **43**, 2609–2645.

Carmignoto G & Vicini S (1992). Activity-dependent decrease in NMDA receptor responses during development of the visual cortex. *Science* **258**, 1007–1011.

Chen N, Luo T & Raymond LA (1999). Subtype-dependence of NMDA receptor channel open probability. *J Neurosci* **19**, 6844–6854.

Clements JD, Lester RA, Tong G, Jahr CE & Westbrook GL (1992). The time course of glutamate in the synaptic cleft. *Science* **258**, 1498–1501.

Colquhoun D & Sigworth FJ (1995). Fitting and statistical analysis of single-channel records. *Single Channel Recording*. Plenum Press New York.

Cull-Candy S, Brickley S & Farrant M (2001). NMDA receptor subunits: diversity, development and disease. *Curr Opin Neurobiol* **11**, 327–335.

Cull-Candy SG & Wyllie DJ (1991). Glutamate-receptor channels in mammalian glial cells. *Ann N Y Acad Sci* **633**, 458–474.

Deisseroth K, Mermelstein PG, Xia H & Tsien RW (2003). Signaling from synapse to nucleus: the logic behind the mechanisms. *Curr Opin Neurobiol* **13**, 354–365.

DeMaria CD, Soong TW, Alseikhan BA, Alvania RS & Yue DT (2001). Calmodulin bifurcates the local Ca^{2+} signal that modulates P/Q-type Ca^{2+} channels. *Nature* **411**, 484–489.

Dingledine R, Borges K, Bowie D & Traynelis SF (1999). The glutamate receptor ion channels. *Pharmacol Rev* **51**, 7–61.

Ehlers MD (2003). Activity level controls postsynaptic composition and signaling via the ubiquitin-proteasome system. *Nat Neurosci* **6**, 231–242.

Erreger K, Chen PE, Wyllie DJA & Traynelis SF (2004). Glutamate receptor gating. *Crit Rev Neurobiol* **16**, 187–225.

Flint AC, Maisch US, Weishaupt JH, Kriegstein AR & Monyer H (1997). NR2A subunit expression shortens NMDA receptor synaptic currents in developing neocortex. *J Neurosci* **17**, 2469–2476.

Fujisawa S & Aoki C (2003). In vivo blockade of N-methyl-D-aspartate receptors induces rapid trafficking of NR2B subunits away from synapses and out of spines and terminals in adult cortex. *Neuroscience* **121**, 51–63.

Gibb AJ (2004). NMDA receptor subunit gating – uncovered. *Trends Neurosci* **27**, 7–10.

Gibb AJ & Colquhoun D (1991). Glutamate activation of a single NMDA receptor-channel produces a cluster of channel openings. *Proc R Soc Lond B Biol Sci* **243**, 39–45.

Hestrin S (1992). Developmental regulation of NMDA receptor-mediated synaptic currents at a central synapse. *Nature* **357**, 686–689.

Hrabetova S, Serrano P, Blace N, Tse HW, Skifter DA, Jane DE, Monaghan DT & Sacktor TC (2000). Distinct NMDA receptor subpopulations contribute to long-term potentiation and long-term depression induction. *J Neurosci* **20**, RC81.

Jackson MB, Wong BS, Morris CE, Lecar H & Christian CN (1983). Successive openings of the same acetylcholine receptor channel are correlated in open time. *Biophys J* **42**, 109–114.

Jahr CE (1992). High probability opening of NMDA receptor channels by L-glutamate. *Science* **255**, 470–472.

Jin R, Banke TG, Mayer ML, Traynelis SF & Gouaux E (2003). Structural basis for partial agonist action at ionotropic glutamate receptors. *Nat Neurosci* **6**, 803–810.

Karpen JW & Ruiz M (2002). Ion channels: does each subunit do something on its own? *Trends Biochem Sci* **27**, 402–409.

Krupp JJ, Vissel B, Heinemann SF & Westbrook GL (1998). N-terminal domains in the NR2 subunit control desensitization of NMDA receptors. *Neuron* **20**, 317–327.

Kutsuwada T, Sakimura K, Manabe T, Takayama C, Katakura N, Kushiya E *et al.* (1996). Impairment of suckling response, trigeminal neuronal pattern formation, and hippocampal LTD in NMDA receptor epsilon 2 subunit mutant mice. *Neuron* **16**, 333–344.

Li B, Chen N, Luo T, Otsu Y, Murphy TH & Raymond LA (2002). Differential regulation of synaptic and extra-synaptic NMDA receptors. *Nat Neurosci* **5**, 833–834.

Liu L, Wong TP, Pozza MF, Lingenhoehl K, Wang Y, Sheng M, Auberson YP & Wang YT (2004). Role of NMDA receptor subtypes in governing the direction of hippocampal synaptic plasticity. *Science* **304**, 1021–1024.

Magleby KL (2004). Modal gating of NMDA receptors. *Trends Neurosci* **27**, 231–233.

Massey PV, Johnson BE, Moult PR, Auberson YP, Brown MW, Molnar E, Collingridge GL & Bashir ZI (2004). Differential roles of NR2A and NR2B-containing NMDA receptors in cortical long-term potentiation and long-term depression. *J Neurosci* **24**, 7821–7828.

Monyer H, Burnashev N, Laurie DJ, Sakmann B & Seeburg PH (1994). Developmental and regional expression in the rat brain and functional properties of four NMDA receptors. *Neuron* **12**, 529–540.

Paoletti P, Perin-Dureau F, Fayyazuddin A, Le Goff A, Callebaut I & Neyton J (2000). Molecular organization of a zinc binding n-terminal modulatory domain in a NMDA receptor subunit. *Neuron* **28**, 911–925.

Popescu G & Auerbach A (2003). Modal gating of NMDA receptors and the shape of their synaptic response. *Nat Neurosci* **6**, 476–483.

Popescu G, Robert A, Howe JR & Auerbach A (2004). Reaction mechanism determines NMDA receptor response to repetitive stimulation. *Nature* **430**, 790–793.

Premkumar LS, Qin F & Auerbach A (1997). Subconductance states of a mutant NMDA receptor channel kinetics, calcium, and voltage dependence. *J Gen Physiol* **109**, 181–189.

Qin F (2004). Restoration of single-channel currents using the segmental k-means method based on hidden Markov modeling. *Biophys J* **86**, 1488–1501.

Qin F, Auerbach A & Sachs F (1997). Maximum likelihood estimation of aggregated Markov processes. *Proc R Soc Lond B Biol Sci* **264**, 375–383.

Rosenmund C, Stern-Bach Y & Stevens CF (1998). The tetrameric structure of a glutamate receptor channel. *Science* **280**, 1596–1599.

Rumbaugh G & Vicini S (1999). Distinct synaptic and extrasynaptic NMDA receptors in developing cerebellar granule neurons. *J Neurosci* **19**, 10603–10610.

Schneggenburger R (1996). Simultaneous measurement of Ca^{2+} influx and reversal potentials in recombinant N-methyl-D-aspartate receptor channels. *Biophys J* **70**, 2165–2174.

Sheng M, Cummings J, Roldan LA, Jan YN & Jan LY (1994). Changing subunit composition of heteromeric NMDA receptors during development of rat cortex. *Nature* **368**, 144–147.

Smith TC & Howe JR (2000). Concentration-dependent substate behavior of native AMPA receptors. *Nat Neurosci* **3**, 992–997.

Sucher NJ, Awobuluyi M, Choi YB & Lipton SA (1996). NMDA receptors: from genes to channels. *Trends Pharmacol Sci* **17**, 348–355.

Tovar KR & Westbrook GL (1999). The incorporation of NMDA receptors with a distinct subunit composition at nascent hippocampal synapses in vitro. *J Neurosci* **19**, 4180–4188.

Vicini S, Wang JF, Li JH, Zhu WJ, Wang YH, Luo JH, Wolfe BB & Grayson DR (1998). Functional and pharmacological differences between recombinant N-methyl-D-aspartate receptors. *J Neurophysiol* **79**, 555–566.

Williams K, Zappia AM, Pritchett DB, Shen YM & Molinoff PB (1994). Sensitivity of the N-methyl-D-aspartate receptor to polyamines is controlled by NR2 subunits. *Mol Pharmacol* **45**, 803–809.

Yoshimura Y, Ohmura T & Komatsu Y (2003). Two forms of synaptic plasticity with distinct dependence on age, experience, and NMDA receptor subtype in rat visual cortex. *J Neurosci* **23**, 6557–6566.

van Zundert B, Yoshii A & Constantine-Paton M (2004). Receptor compartmentalization and trafficking at glutamate synapses: a developmental proposal. *Trends Neurosci* **27**, 428–437.

Acknowledgements

We thank Dr Morris Benveniste and Dr Raymond Dingledine for helpful discussions and commentary on the project. We thank Phuong Le, Polina Lyuboslavsky and Antoine Almonte for excellent technical assistance. This work was supported by The Howard Hughes Medical Institute (K.E.), the National Institutes of Health (National Institute of Neurological Disorders and Stroke NS36654, S.T.), National Alliance for Research on Schizophrenia and Depression (S.T.) and the Biotechnology and Biological Sciences Research Council (D.J.A.W.).